

Field-controlled suppression of phonon-induced transitions in coupled quantum dots

Andrea Bertoni^{a)} and Massimo Rontani

INFN National Research Center on nanoStructures and bioSystems at Surfaces (S3), Via Campi 213/A, 41100 Modena, Italy

Guido Goldoni, Filippo Troiani, and Elisa Molinari

INFN National Research Center on nanoStructures and bioSystems at Surfaces (S3), Modena, Italy and Dipartimento di Fisica, Università di Modena e Reggio Emilia, Italy

(Received 10 June 2004; accepted 27 September 2004)

We suggest that order-of-magnitude reduction of the longitudinal-acoustic phonon scattering rate, the dominant decoherence mechanism in quantum dots, can be achieved in coupled structures by the application of an external electric or magnetic field. Modulation of the scattering rate is traced to the relation between the wavelength of the emitted phonon and the length scale of delocalized electron wave functions. Explicit calculations for realistic devices, performed with a Fermi golden rule approach and a fully three-dimensional description of the electronic quantum states, show that the lifetime of specific states can achieve tens of microseconds. Our findings extend the feasibility basis of many proposals for quantum gates based on coupled quantum dots. © 2004 American Institute of Physics. [DOI: 10.1063/1.1818345]

The loss of quantum coherence, brought about by the coupling between charge degrees of freedom and lattice vibrations, constitutes a main limitation for single and coupled quantum dot (SQD and CQD) implementations of quantum logic gates, as well as for a wide class of novel few- and single-electron devices. In quantum dots (QDs)¹ the discrete nature of the energy spectrum strongly reduces this interaction with respect to other semiconductor systems. In particular, the coupling with the dispersionless optical phonons, the main source of decoherence in structures of higher dimensionality, is either completely suppressed² or, in specific conditions, leads to localized polaronic states.³ Still, however, emission of longitudinal acoustic (LA) phonons⁴ limits the charge coherence times to tens of nanoseconds in typical devices, since intraband electronic transitions merge into the LA phonon continuum. Tailoring the coupling between electronic quantum states and LA phonons would be a fundamental step toward the design of quantum devices with optimal operation conditions.

In this letter we show that LA-phonon scattering rate of specific transitions can be suppressed in CQDs by proper structure design (as already discussed in Ref. 5 for quantum dot arrays) and by use of external magnetic and electric fields. This is accomplished by exploiting the interplay between the wave vector of the emitted or absorbed phonon and the length scale of the quantum states. While the above-noted effect is small in typical SQDs, which are characterized by a single length scale, we show that order-of-magnitude modulation of the scattering rate can be achieved in coherently coupled QDs, where two characteristic length scales come into play, namely the dimension of each dot and the dimension of the CQD system as a whole.

Decay times of a single electron in a SQD have been measured recently by transport spectroscopy.⁶ These experiments, which specifically probe the decay of carriers injected in the first excited state to the ground state, showed a satis-

factory agreement with a Fermi golden rule estimate of the electron relaxation times. In the following we investigate the decay time of specific low energy transitions which are, therefore, directly accessible with similar techniques. As a prototypical system, we consider a GaAs/AlGaAs CQD structure formed by two identical QDs with cylindrical shape, coupled along the growth direction.⁷ We describe the electronic quantum states within the familiar envelope function approximation and consider a parabolic confinement in the xy plane of the cylinders, and a symmetric double-well in the z direction: $V(\mathbf{r}) = V_z(z) + \frac{1}{2}m\omega_0^2(x^2 + y^2)$ where $V_z(z) = V_l$ if $L_b/2 \leq |z| \leq (L_b/2 + L_d)$ and $V_z(z) = V_h$ otherwise. Here L_d is the thickness of the GaAs layers and L_b is the thickness of the interdot layer. $(V_h - V_l)$ is the band offset of GaAs/AlGaAs. Furthermore, we consider either a magnetic (B) or an electric (E) field applied in the z direction. For this cylindrically symmetric configuration, the eigenfunctions can be given the separable form $\psi_{nmg}(\mathbf{r}) = \phi_{nm}(x, y)\chi_g(z)$, with $n=0, 1, \dots$ the radial and $m=0, \pm 1, \dots$ the angular quantum number of the Fock–Darwin state $\phi_{nm}(x, y)$; $g=0$ (1) indicates the ground (first excited) eigenstate for the biased double-well potential along the z direction.

We use the standard deformation-potential model for the electron–LA phonon interaction, with the interaction Hamiltonian $\mathbf{H}_{e-p} = \sum_{\mathbf{q}} F(\mathbf{q})(b_{\mathbf{q}}e^{i\mathbf{q}\mathbf{r}} + b_{\mathbf{q}}^\dagger e^{-i\mathbf{q}\mathbf{r}})$, where $b_{\mathbf{q}}$ and $b_{\mathbf{q}}^\dagger$ are the annihilation and creation operators for a LA-phonon with wave vector \mathbf{q} and $F(\mathbf{q}) = q\sqrt{\hbar D^2/(2\rho\omega_{\mathbf{q}}V)}$. D is the deformation potential, ρ is the crystal density, and V the volume of the system. A linear dispersion approximation $\omega_{\mathbf{q}} = vq$ is used for the LA branch, with v longitudinal sound speed.⁸ Furthermore, we assume that the device operates in a single-electron regime: electron–electron scattering is neglected accordingly.

In the following we shall concentrate on the scattering rate between specific excited (initial) states ψ_i , with energy E_i , and the ground (final) state ψ_f , with energy E_f .⁹ The scattering rate at zero temperature, given by the Fermi golden

^{a)}Electronic mail: bertoni.andrea@unimore.it

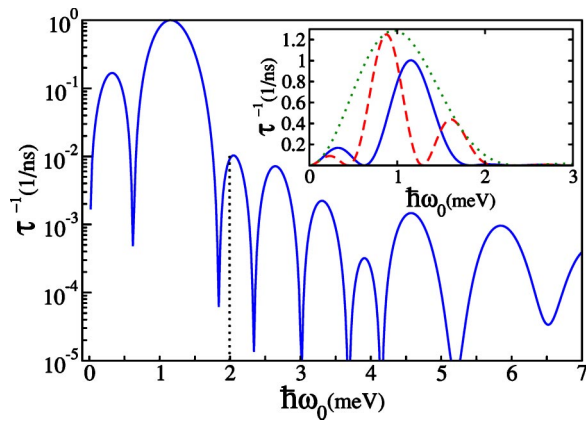


FIG. 1. (Color online) Scattering rate in a CQD ($L_d=10$ nm, $L_b=3$ nm) for the transition $(n, m, g)=(0, -1, 0) \rightarrow (0, 0, 0)$ as a function of the in-plane parabolic confinement energy $\hbar\omega_0$. The dotted line shows the value of $\hbar\omega_0$ used for the simulations with an applied magnetic field. Inset: the scattering rate for the same sample is compared with that for a CQD with a larger barrier ($L_b=8$ nm, dashed curve) and for a SQD ($L_d=10$ nm, dotted curve), in a linear scale.

rule, is $\tau^{-1} = (2\pi/\hbar) \sum_{\mathbf{q}} |F(q)M_{fi}(\mathbf{q})|^2 \delta(E_f - E_i + \hbar\omega_{\mathbf{q}})$, where $M_{fi}(\mathbf{q}) = \langle \psi_f | e^{-i\mathbf{q}r} | \psi_i \rangle$.

It is convenient to write the phonon wave vector \mathbf{q} in spherical coordinates and separate the scattering matrix $M_{fi}(\mathbf{q})$ into a z component $M_{fi}^{(z)}(q_z = q \cos \theta)$, to be evaluated numerically, and an in-plane component $M_{fi}^{(xy)}(q_x = q \cos \varphi \sin \theta, q_y = q \sin \varphi \sin \theta)$ which can be exactly derived.¹⁰ Performing the integration over q , one finally obtains:

$$\tau^{-1} = \frac{q_0^2}{v(2\pi\hbar)^2} F(q_0) \int_0^{2\pi} d\varphi \int_0^{\pi/2} d\theta \sin \theta \times |M_{fi}^{(z)}(q_0 \cos \theta) M_{fi}^{(xy)}(q_0 \cos \varphi \sin \theta, q_0 \sin \varphi \sin \theta)|^2, \quad (1)$$

with $q_0 = (E_i - E_f)/(\hbar v)$. We emphasize that the decoupling of the in-plane and vertical degrees of freedom in Eq. (1) is approximately valid as long as the in-plane and vertical confinement have different length scales, as is achieved by many growth techniques.

Now we focus on the $(n, m, g)=(0, -1, 0) \rightarrow (0, 0, 0)$ transition, which only involves in-plane degrees of freedom. We choose a CQD system (see Fig. 1, caption) such that the tunneling energy is larger than $\hbar\omega_0$ and $(0, -1, 0)$ is the lowest excited state. Figure 1 shows the computed scattering rate at $B=0$ T and zero temperature as a function of the in-plane confining energy $\hbar\omega_0$. The striking oscillations, which cover several orders of magnitude, have their origin in the phase relation between the phonon plane wave corresponding to the considered electronic transition and the electron wave function delocalized between the two QDs: two limiting conditions, one with maximum overlap, the other with minimum overlap, due to electron-phonon antiphase, occur repeatedly as the confinement energy (and, therefore, the energy of the matching phonon) is varied; the two cases correspond to a maximum and a minimum of the matrix element $M_{fi}^{(z)}$, respectively. In the inset of Fig. 1 we compare the scattering rate of two CQD structures, with different barrier widths, with the one of a SQD. As one may expect, the curves have a similar limiting behavior: when the confining potential and,

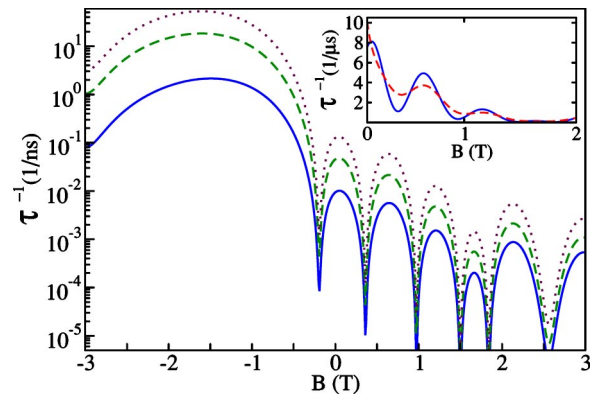


FIG. 2. (Color online) Scattering rate in a CQD ($L_d=10$ nm, $L_b=3$ nm, $\hbar\omega_0=2$ meV) for the transition $(n, m, g)=(0, -1, 0) \rightarrow (0, 0, 0)$ (Ref. 11) as a function of the applied vertical magnetic field B (see the text) at three temperatures, $T=0$ K (solid), 100 K (dashed), 300 K (dotted). The proper Bose statistics for phonon modes has been used in the latter two simulations. Inset: two different energy-uncertainty conditions are compared at $T=0$ K: the data are convoluted with a Gaussian uncertainty of about 10% (FWHM=0.2 meV, solid line) and 20% (FWHM=0.4 meV, dashed line) on the dot confining energy.

as a consequence, the energy of the emitted phonon is very low, τ^{-1} decreases due to (a) the q^2 prefactor ensuing from the low-energy LA-phonon density of states and the linear q dependence of $F(q)$ in Eq. (1), and (b) the decreasing value of $M_{fi}^{(xy)}(\mathbf{q})$ due to orthogonality of the states (at vanishing q the electron-phonon Hamiltonian becomes constant). In the opposite limit, for $\hbar\omega_0 > 2$ meV, the phonon oscillation length becomes much smaller than the typical length scale of the electron wave function; as a consequence $M_{fi}(\mathbf{q})$ vanishes since the initial and final electron states do not possess the proper Fourier component able to trigger the phonon oscillation. In the *intermediate regime*, while the SQD curve shows a single well-defined maximum, the CQD curve oscillates. The oscillation pattern depends on the geometry of the system.⁵ If the distance between the dots is increased, the energy difference between the maxima decreases (see inset in Fig. 1), with the CQD curve enveloped by the SQD curve.

The modulation shown in Fig. 1 is obtained by changing the lateral confining potential, i.e., a structure parameter that could be hardly tuned in an experimental setup. We show in the following that the strong suppression of acoustic-phonon induced scattering can also be driven by a magnetic field B parallel to the growth direction. Indeed, B induces (a) a non-uniform shift in the energies E_i and E_f and, consequently, a shift in the emitted phonon wave vector q_0 ; (b) a modification of the in-plane scattering matrix $M_{fi}^{(xy)}$ originating from the stronger localization of the wave functions. Figure 2 shows that, for a CQD with a 2 meV confining energy, the acoustic-phonon scattering rate is reduced by four orders of magnitude at $B=1$ T. In order to test the robustness of this effect in realistic experimental conditions, and particularly to compare with possible pump-and-probe experiments,⁶ in which the electron energy could vary between the cycles leading to a finite energy uncertainty, we introduced a Gaussian smearing in the QD confining energy. The resulting scattering rate (Fig. 2, inset) still shows oscillations of about one order of magnitude when an uncertainty of 0.2 meV is assumed.

Next, we analyze the transition rate between two different pseudospin levels, $(n, m, g)=(0, 0, 1) \rightarrow (0, 0, 0)$, i.e.,

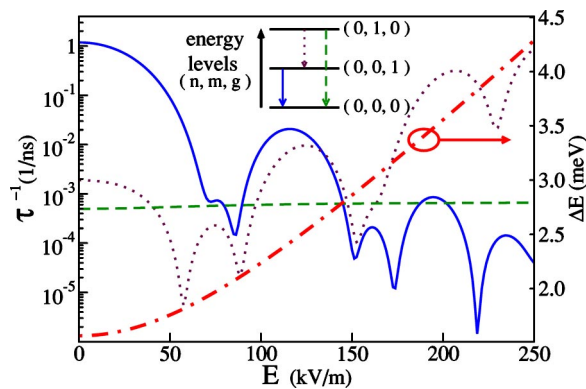


FIG. 3. (Color online) Scattering rate (solid line), for the lowest pseudospin transition $(n, m, g) = (0, 0, 1) \rightarrow (0, 0, 0)$ in a CQD with $L_d = 12$ nm, $L_b = 4$ nm, and $\hbar\omega_0 = 5$ meV as a function of an electric field applied along z . The scattering rate for $(0, 1, 0) \rightarrow (0, 0, 1)$ and $(0, 1, 0) \rightarrow (0, 0, 0)$ are shown with dotted and dashed lines, respectively. The energy of the emitted LA phonon is reported for reference (thick dash-dotted curve, right axis).

with the z component of the electron wave function decaying from the first excited to the ground state. We consider a sample with $\hbar\omega_0$ substantially larger than the tunneling energy, so that the above transition is the lowest (see Fig. 3, caption). In this case the wavelength of the emitted phonon is controlled by the tunneling energy, that can be tuned by means of an electric field applied in the z direction. As in the previous cases, order-of-magnitude modulation of the lowest transition can be achieved at specific fields (Fig. 3, solid line); furthermore, scattering rates tend to be smaller at higher fields as a result of increasing the wave vector of the emitted phonon, whose energy is also shown. Note that the effect of the fields on the scattering rates generally depends on the specific transition, therefore making it possible to tailor the scattering rates and to make only specific states robust to phonon-induced decoherence. This should allow a selective population of excited states. As an example, in Fig. 3 we report the scattering rates of the second excited state to the lower ones (see inset): at $E \sim 200$ kV/m $(0, 1, 0)$ decays preferentially to $(0, 0, 1)$ which, in turn, is long lived. Finally, we remark that the observation of the field-dependent oscillation

of the transition rate would serve as a signature for the coherent delocalization of electron states in CQDs.

In summary we have shown that a strong suppression of LA-scattering, the main source of electron decoherence in quasi-zero-dimensional systems, can be obtained in CQDs with energy-level separation around 3 meV. Significantly, the relaxation time can be controlled by external magnetic or electric field and increased up to tens of μ s; this should be compared to SQDs with similar level spacing, where scattering times are of the order of nanoseconds and not strongly affected by external fields.

This work has been partially supported by Projects MIUR-FIRB No. RBAU01ZEML, MIUR-COFIN No. 2003020984, INFN Calcolo Parallelo 2004, and MAE, Dir. Gen. Promozione Cooperazione Culturale.

¹L. Jacak, P. Hawrylak, and A. Wójs, *Quantum Dots* (Springer, Berlin, 1998); W. G. van der Wiel, S. D. Franceschi, J. M. Elzerman, T. Fujisawa, S. Tarucha, and L. P. Kouwenhoven, *Rev. Mod. Phys.* **75**, 1 (2003); S. M. Reimann and M. Manninen, *ibid.* **74**, 1283 (2002).

²U. Bockelmann and G. Bastard, *Phys. Rev. B* **42**, 8947 (1990).

³T. Inoshita and H. Sakaki, *Phys. Rev. B* **56**, R4355 (1997); S. Hameau, Y. Guldner, O. Verzele, R. Ferreira, G. Bastard, J. Zeman, A. Lemaître, and J. M. Gérard, *Phys. Rev. Lett.* **83**, 4152 (1999).

⁴L. Jacak, P. Machnikowski, J. Krasnyj, and P. Zoller, *Eur. Phys. J. D* **22**, 319 (2003).

⁵P. Zanardi and F. Rossi, *Phys. Rev. Lett.* **81**, 4752 (1998).

⁶T. Fujisawa, D. G. Austing, Y. Tokura, Y. Hirayama, and S. Tarucha, *Nature (London)* **419**, 278 (2002).

⁷S. Tarucha, D. G. Austing, T. Honda, R. J. van der Hage, and L. P. Kouwenhoven, *Phys. Rev. Lett.* **77**, 3613 (1996); M. Rontani, S. Amaha, K. Muraki, F. Manghi, E. Molinari, S. Tarucha, and D. G. Austing, *Phys. Rev. B* **69**, 085327 (2004).

⁸In the numerical simulations we consider a GaAs/Al_{0.3}Ga_{0.7}As heterostructure and use the following parameters: $D = 8.6$ eV, $\rho = 5300$ kg/m³, $v = 3700$ m/s, $V_h - V_l = 243$ meV.

⁹The subscripts i and f indicate, in compact notation, the three quantum numbers (n_i, m_i, g_i) and (n_f, m_f, g_f) of the initial and final state, respectively.

¹⁰U. Bockelmann, *Phys. Rev. B* **50**, 17271 (1994).

¹¹At negative B $(0, -1, 0)$ is higher than $(0, 1, 0)$; the $(0, 1, 0) \rightarrow (0, 0, 0)$ scattering rate can be inferred from that of $(0, -1, 0) \rightarrow (0, 0, 0)$, reported in Fig. 2, by changing the sign of the field B .